Receptor polarization through localized activity and global sensitization

Andrew Goetz
Department of Biomedical Engineering, Yale University, New Haven, CT 06511

Purushottam D. Dixit
*Department of Biomedical Engineering, Yale University, New Haven, CT 06511 and Systems Biology Institute, Yale University, West Haven, CT 06516**

Abstract: Eukaryotic cells *chemosense* concentration gradients of extracellular ligands using membrane-bound receptors that polarize their activity. Receptors from several chemosensing families are preferentially degraded after activation and undergo significant lateral diffusion, both of which may blunt their polarization. To explore the combined role of these two seemingly detrimental phenomena on active receptor polarization, we use a reaction/diffusion model. The model elucidates a counterintuitive principle that governs receptor polarization under external gradients: Localized Activity and Global Sensitization (LAGS). In LAGS, receptor activity is localized through receptor degradation or ligand unbinding. In contrast, uniform sensitivity to ligands is maintained over the plasma membrane through lateral receptor diffusion. Surprisingly, increasing preferential degradation of active receptors and increasing lateral diffusion of all receptors both sharpen active receptor polarization. Additionally, when combined with receptor oligomerization, an increase in preferential degradation allows cells to sense relative ligand gradients over a larger range of background ligand concentrations. An analytical model identifies parameter regimes that dictate which processes dominate receptor polarization. A survey of kinetic parameters suggests that receptor polarization in many mammalian pathways can be modeled using LAGS.

I. INTRODUCTION

Unicellular organisms and cells of multicellular organisms have developed intricate ways to navigate their spatially inhomogeneous environment. For example, many prokaryotic organisms can climb up/down the gradients of attractants/repellents through temporal integration in a run-and-tumble motion [1, 2]. Similarly, unicellular eukaryotes such as yeast use spatially inhomogeneous chemical cues to identify the location of mates [3]. Cells of metazoans also partake in spatially inhomogeneous behaviors including chemotaxis [4–6] and growth and development [7, 8].

Small prokaryotic cells often use spatial exploration and temporal averaging to gauge local ligand concentrations [1, 2]. Several studies have explored the limits of directional chemosensing by ligand-cognate receptors on prokaryotic cells. These studies have highlighted the strategies employed by cells to overcome fluctuations in ligand concentrations and to infer accurate chemical gradients [9–14]. In contrast to prokaryotes, the first step in gradient-induced asymmetric behaviors by eukaryotic cells is receptor polarization; ligand-cognate receptors on the cells' plasma membrane bind to ligands and create a spatially inhomogeneous partitioning of the activated receptors aligned with the ligand gradient [15, 16]. In eukaryotic cells, significant attention has been spent on understanding processes downstream of receptor-ligand interactions [4, 17–23]. Notably, the role of processes at the plasma membrane including receptor diffusion and trafficking in modulating receptor polarization has received less attention [24, 25].

A common feature of many eukaryotic signaling networks, including several chemosensing receptors families such as receptor tyrosine kinases (RTKs) [26, 27], G-protein coupled receptors (GPCRs) [28], and cytokine receptors [29, 30], is preferential endocytosis and subsequent degradation of ligand-bound activated receptors. A primary function of preferential degradation is thought to be downregulation of receptor activity [31–33]. In addition to preferential degradation, cell surface receptors undergo lateral diffusion on the plasma membrane [34–37]. Often, activated receptors diffuse at a slower rate, potentially due to receptor oligomerization, receptor-effector complex formation or both [35, 37]. Nonetheless, lateral diffusion spreads out receptors on the membrane, which may potentially blunt their ligand-induced polarization as well.

In this work, we show how these two ubiquitous processes, degradation and diffusion, that are potentially a corruptive influence on receptor polarization synergize to enhance it. To that end, we employ an idealized one dimensional reaction diffusion model of receptors-ligand signaling. Counterintuitively, the model suggests that increasing lateral diffusion of receptors and increasing preferential degradation of active receptors sharpens the their polarization. We also find that preferential degradation, in combination with receptor oligomerization, endows the signaling network with the ability to perform fold change detection (Weber-Fechner law) in ligand concentrations [38, 39] over a large range of background ligand concentrations. Moreover, in the presence of basal receptor activation [40, 41], the signaling network becomes capable of discerning the local ligand input relative to

* email: purushottam.dixit@yale.edu

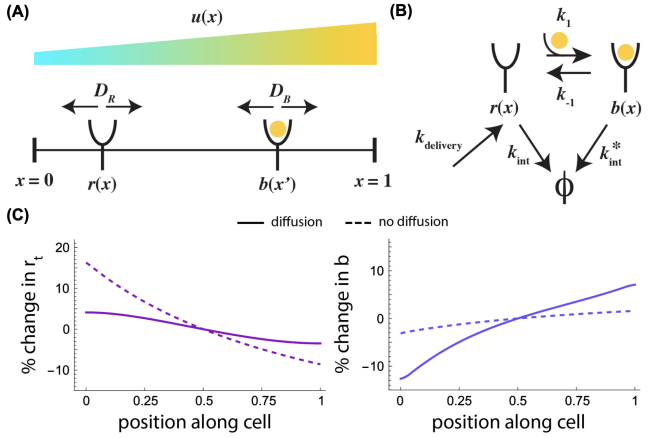

FIG. 1. **Simple model elucidates LAGS.** (A) Ligand-free and ligand-bound receptors diffuse along the cell surface between dimensionless coordinates $x = 0$ and $x = 1$ with diffusion constants D_R and D_B, respectively. (B) Reactions that take place at every location x in the model. (C) Profiles of the total receptors, r_t, and active receptors, b, along the cell with diffusion ($\gamma = 1$) and without diffusion ($\gamma \ll 1 = 10^{-4}$) of receptors. For both cases, we set $\delta = 1$, $\mu = 2000$ [39], and $\beta = 10$ [26]. See main text for definitions of dimensionless quantities. The extracellular concentration profile of the ligand was set to $u(x) = u_0(1 + gx)$ where $u_0 = 1$ and $g = 0.1$.

the average input along the cell, an essential property for chemosensing circuits [18]. Finally, an analytical simplification of the model identifies parameter regimes that dictate which processes govern receptor polarization.

These effects together highlight a novel principle governing receptor polarization: Localized Activity and Global Sensitization (LAGS). In LAGS, receptor activity remains localized through a combination of fast ligand dissociation and preferential degradation. In contrast, a uniform sensitivity to ligands is maintained through lateral diffusion of receptors. A survey of relevant kinetic parameters for many mammalian receptor systems suggests that LAGS is a generally applicable principle to understand receptor polarization.

II. RESULTS

A. A one dimensional reaction diffusion model describes receptor polarization

To investigate the combined role of receptor diffusion and degradation on polarization, we consider a one dimensional reaction diffusion model of ligand-mediated signaling that captures key features of receptor signaling pathways such as RTKs and GPCRs. The model imagines a one-dimensional cell surface that exists between $X = 0$ and $X = l_C$ where l_C is the length of the cell. We imagine two types of receptors: ligand-free receptors R and ligand-bound active receptors B. The position-dependent concentrations of the receptors are denoted by $R(X)$ and $B(X)$ respectively. We denote the externally imposed gradient of the ligand as $L(X)$. For simplicity, we assume that the ligand gradient is not perturbed through interactions with the cell. In many eukaryotic signaling networks, the number of ligand-cognate receptors ranges between $10^4 - 10^6$ molecules per cell [42–45]. Focusing on those pathways, we develop our model in the deterministic regime. We leave it for future studies to investigate the role of stochastic noise in ligand fluctuations and receptor trafficking.

The schematic of the model is shown in Figures 1A and 1B. Briefly, receptors associate with the ligand at a rate k_1 and ligand bound receptors dissociate from the ligand at a rate k_{-1}. Ligand-free receptors are delivered to the cell surface at a constant rate k_{delivery} and removed from the cell surface at a rate k_{int} and degraded. A key component of many eukaryotic signaling networks is preferential endocytosis and degradation of activated receptors [26, 27]. Consequently, in the model, we assume that ligand-bound receptors (along with the ligand) are degraded at a faster rate $k^*_{\text{int}} > k_{\text{int}}$. Finally, diffusion constants for ligand-free and ligand-bound receptors are denoted by D_R and D_B.

Before writing down model equations, we recognize several dimensionless parameters and concentrations. We recognize $x = X/l_C$ as the dimensionless length, $u(x) = L(x)k_{-1}/k_1$ as the dimensionless ligand concentration, and $\tau = 1/k_{\text{int}}$ as dimensionless time. We also recognize $R_0 = k_{\text{delivery}}/k_{\text{int}}$ as the number of receptors in the absence of the ligand and introduce normalized receptor concentrations $r(x) = R(x)/R_0$ and $b(x) = B(x)/R_0$. We also recognize: (1) $\beta = k^*_{\text{int}}/k_{\text{int}}$, the dimensionless degradation rate of activated receptors, (2) $\gamma = D_R/(k_{\text{int}} * l_C^2)$, the dimensionless diffusion constant of inactive receptors, (3) $\delta = D_R/D_B$, the ratio of diffusion constants of active and inactive receptors, and (4) $\mu = k_{-1}/k_{\text{int}}$, the dimensionless ligand unbinding rate. With these definitions, the reaction diffusion equations describing the receptors are given by:

$$\begin{aligned} \frac{\partial r(x)}{\partial \tau} &= \gamma \frac{\partial^2 r(x)}{\partial x^2} + 1 - r(x) - \mu u(x) r(x) + \mu b(x) \\ \frac{\partial b(x)}{\partial \tau} &= \frac{\gamma}{\delta} \frac{\partial^2 b(x)}{\partial x^2} - \beta b(x) + \mu u(x) r(x) - \mu b(x) \end{aligned} \tag{1}$$

While Eqs. 1 provide a full description of our model, an intuitive simplification is obtained when ligand binding is significantly faster than receptor internalization ($\mu \gg 1$) and receptor diffusion is independent of receptor activity ($\delta = 1$). Under these conditions, ligand bound and ligand free receptors at any location x equilibrate instantaneously with the local ligand concentration $u(x)$. Here, we have

$$r(x) = \frac{r_t(x)}{u(x) + 1} \text{ and } b(x) = \frac{r_t(x) u(x)}{u(x) + 1}. \tag{2}$$

In Eq. 2, $r_t(x)$ is the total number of receptors whose

time evolution is governed by:

$$\frac{\partial r_t(x)}{\partial \tau} = 1 - \frac{1+\beta u(x)}{1+u(x)} r_t(x) + \gamma \frac{\partial^2}{\partial x^2} r_t(x). \quad (3)$$

In Eq. 3, the individual terms on the right hand side represent receptor production, receptor degradation, and receptor diffusion respectively.

Throughout the manuscript, we assume that extracellular spatial ligand gradients are small and can be represented as

$$u(x) = u_0(1 + gx) \quad (4)$$

where u_0 is the background ligand concentration and g is the relative gradient. Without loss of generality, we assume that the $x = 0$ side of the cell is exposed to the lower concentration. Going forward, unless specified otherwise, we will use literature-derived and model-fit estimates of our dimensionless parameters based on previous work on the EGFR pathway. Unless specified otherwise, we will use $\beta = 40$ [39], $\gamma = 0.4$ [35, 37, 39], and $\mu = 2000$ [39]. To disentangle the roll of differential diffusion of receptor species, we will use $\delta = 1$. We solve Eqs. 1 at steady state.

The metric of active receptor polarization (ARP) is defined as the difference ARP $= b(1) - b(0)$ in active receptors between the leading edge and the trailing edge of the cell. Additionally, we also quantify relative receptor polarization which is the relative change $b(1)/b(0)$ in receptor activity between the leading edge and the trailing edge of the cell. Notably, in addition to dimensionless kinetic parameters, ARP (and relative ARP) also depends on background ligand concentration u_0. Unless the dependence on background ligand levels u_0 is explicitly mentioned, we use polarization metrics averaged over a range of background ligand concentrations (see Supplementary Materials).

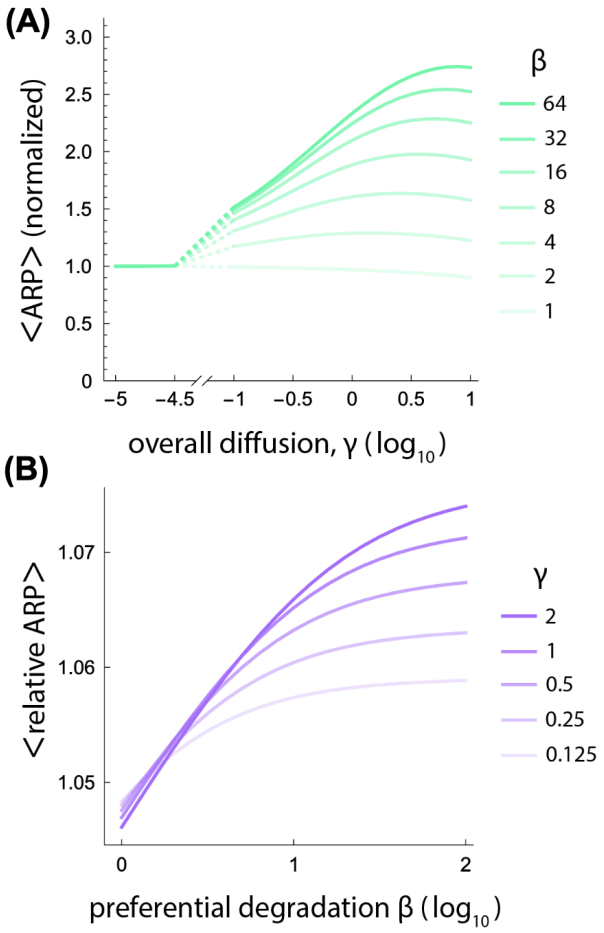

FIG. 2. **Impact of receptor diffusion and degradation on polarization.** (A) Change in ⟨ARP⟩ with an increase in receptor diffusion with different levels of preferential degradation. We set $\delta = 1$ and $\mu = 2000$. For each β (green lines) we report ⟨ARP⟩ normalized to the low diffusion limit ($\gamma \ll 1$). (B) The relative ARP increases with increasing preferential degradation, an effect that is more pronounced at higher diffusion.

B. Diffusion and degradation enhance polarization

In the presence of preferential degradation of activated receptors ($\beta > 1$), we find that lateral diffusion impacts activated receptors (and therefore the ⟨ARP⟩) differently compared to the profile of all receptors (Figure 1C). As expected, diffusion diminishes the spatial gradient of the total receptor level ($r_t = r + b$) along the cell. In contrast, ⟨ARP⟩ increases in the presence of diffusion, an effect seemingly uncharacteristic of diffusion which is expected to erode positional encoding of ligand concentration.

This counterintuitive effect is an essential feature of LAGS. To rationalize it, we refer to Eq. 3. The second term on the right hand side represents the removal of total receptors r_t, a process whose rate increases with increasing ligand levels when $\beta > 1$. As a result, r_t diminishes with increasing ligand concentration [39]. Receptor depletion significantly diminishes ⟨ARP⟩ through diminishing *net* sensitivity towards the ligand — the total receptor concentration — in the direction of signal gradient. This decline in sensitivity is compensated by receptor diffusion (the third term in Eq. 3) which serves to spread out receptors along the cell, thereby providing a more uniform sensitivity. This global sensitization of the cell surface increases ⟨ARP⟩. Notably, the extent to which diffusion increases ⟨ARP⟩ depends on the intensity of desensitization along the cell in the absence of diffusion. Indeed, Figure 2A shows that cells with higher rates of preferential degradation experience a greater increase in ⟨ARP⟩ from diffusion.

In contrast to diffusion, preferential degradation of active receptors reduces the total number of receptors available for signaling, diminishing ARP. Preferential degradation does however sharpen relative ARP along the cell. This effect is sensitized at higher receptor diffusion (Fig-

ure 2B). To understand how the relative polarization sharpens with increasing β (or γ), we note that an increase in β sharpens the relative gradient of total receptors along the cell. This leads to a stronger γ-dependent compensation of receptor levels in a mechanism similar to the Fick's law of diffusion. This increase in the relative ARP may translate to a stronger polarized response provided there are additional motifs downstream of receptor activity that sense relative changes in receptor levels and not absolute receptor levels. Notably, similar downstream mechanisms have been proposed and validated in the context of temporal ligand sensing by transcription factors [46].

C. Active receptor arrest enhances polarization

In section B, we showed that an increase in overall diffusion enhances $\langle$ARP$\rangle$ in the absence of active receptor arrest. Notably, previous experiments have shown that active and inactive receptors may have different diffusion coefficients [35–37] with the diffusion constant for active receptors smaller than that of inactive receptors. Here, we explore how a difference in diffusion rates between receptor species affects receptor polarization.

Figure 3A shows how active receptor arrest (δ) and overall diffusion (γ) jointly impact $\langle$ARP$\rangle$, revealing two distinct regimes. When overall receptor diffusion is slow (low γ), ARP is sensitive to changes in γ but is insensitive to δ. In this regime, diffusion is weaker than preferential degradation, leading to a strong decline in sensitivity in regions of the cell with high ligand concentration. This decline in sensitivity leads to lower gradient of active receptors along the cell. Consequently, reducing the diffusion of active receptors has only a modest impact on $\langle$ARP$\rangle$. In contrast, at high γ, $\langle$ARP$\rangle$ increases with increasing active receptor arrest (increasing δ) but is largely unaffected by changes in γ. Here, diffusion is effective in spreading out all receptors and specifically reducing the diffusion of active receptors serves to further enhance the sensitivity towards the ligand in regions of the cell with high ligand concentration.

The overall increase in $\langle$ARP$\rangle$ due to active receptor arrest also depends on preferential degradation. $\langle$ARP$\rangle$ is less sensitive to active receptor arrest when preferential degradation is strong (high β) (Figure 3B). This is because at high β, the fraction of total receptors in their active state is lowered at the optimal response background. As a result, arresting the activated receptors has little effect on the net lateral flow of all receptors. Consequently, arrest of active receptors has little effect on the $\langle$ARP$\rangle$. In contrast, when $\beta \sim 1$, receptor concentration equalizes on the cell surface through diffusion. Here, decreasing the diffusion of active receptors serves to aggregate the total receptor count in regions with higher ligand input, thereby increasing sensitivity to the ligand and thus the activity in those regions.

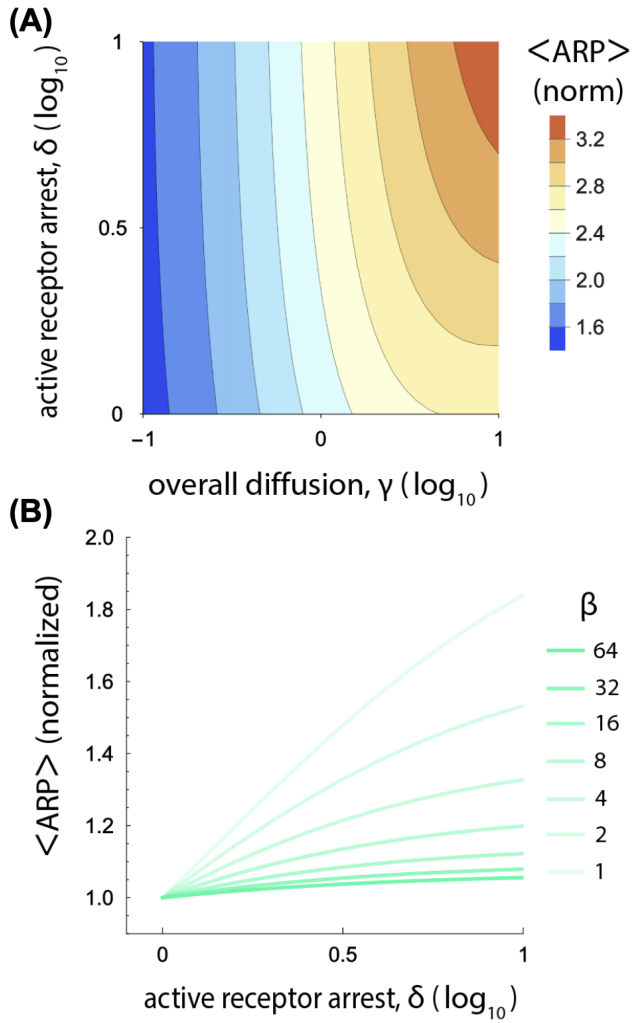

FIG. 3. **Impact of active receptor arrest on $\langle$ARP$\rangle$.** (A) Impact of active receptor arrest and overall diffusion on $\langle$ARP$\rangle$. (B) Impact of active receptor arrest on $\langle$ARP$\rangle$ for different values of β. In panel (A) $\langle$ARP$\rangle$ is normalized to the case where diffusion is low $\gamma \ll 1$. In panel (B), $\langle$ARP$\rangle$ is normalized to the case with no active receptor arrest ($\delta = 1$). Unless stated otherwise we set $\gamma = 0.4$, $\delta = 1$, $\mu = 2000$, and $\beta = 40$.

D. Rapid quenching of active receptor activity shields polarization from diffusion of active receptors

The analysis presented so far assumed a high ligand dissociation rate ($\mu = 2000 \gg 1$). In this limit, active receptors are incapable of carrying their signal laterally along the cell membrane through diffusion as their activity rapidly equilibrates with the local ligand conditions in their new position. This serves to reduce diffusion-driven spread of activity, thereby increasing the $\langle$ARP$\rangle$. While $\mu = 2000$ was chosen from model fits to experimental data on the activity of EGF/EGFR pathway [39], slower binding timescales have been reported in direct experiments [47]. Additionally, receptors may undergo

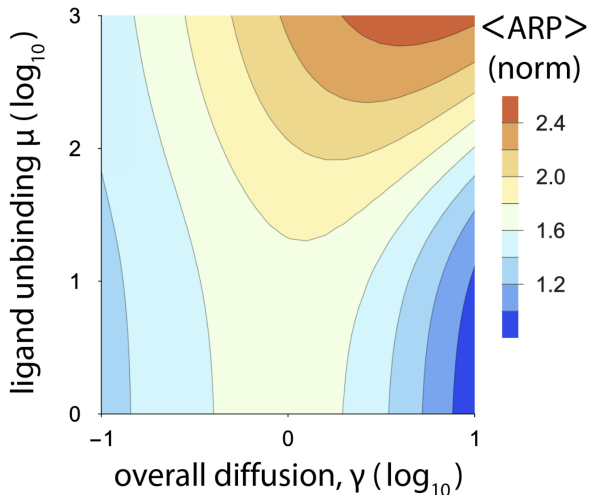

FIG. 4. **Impacts of Ligand Unbinding Rate and Diffusion on** ⟨ARP⟩**.** ⟨ARP⟩ values are nornmalized to the low diffusion limit ($\gamma \ll 1$). We set $\delta = 1$ and $\beta = 40$.

additional processing prior to or after ligand binding (e.g. oligomerization), effectively making loss of activity slower.

Figure 4 shows higher diffusion increases ⟨ARP⟩ when μ is high, as expected from our previous analyses. However, at low values of μ (e.g. $\mu \sim \beta \sim 10 - 50$), ⟨ARP⟩ sharpens with increasing diffusion albeit in a manner that is independent of μ. In this limit, preferential degradation of active receptors *not* their rapid equilibration is the dominant mechanism that prevents lateral propagation of activity. Notably, restricting the loss of information about ligand concentration gradient mirrored in the polarization of active receptors either through rapid re-equilibration or through rapid degradation is a core feature of LAGS. Indeed, in the absence of this restriction (low μ and low β), active receptors diffuse unopposed along the cell, leading to a decrease in ⟨ARP⟩.

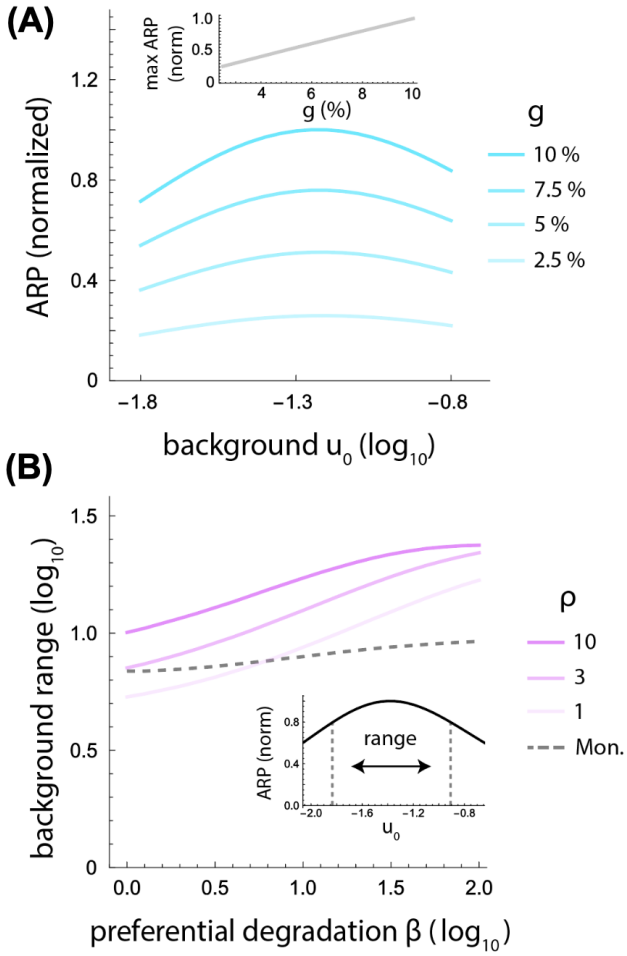

FIG. 5. **Receptor polarization responds to relative changes in ligand concentration.** (A) ARP as a function of background concentrations across different relative gradients. Inset shows how ARP depends on the relative gradient g. ARP is normalized to the maximum response at 10% gradient. (B) The impact of preferential degradation and dimerization on fold change detection range. Unless stated otherwise we set $\gamma = 0.4$, $\delta = 1$, $\mu = 2000$, and $\beta = 40$.

E. Receptor polarization responds to relative changes in ligand concentration

Detection of *relative* not absolute changes in extracellular inputs, also known as fold change detection (FCD), enables cells to remain sensitive under a wide range of background levels [38, 39, 48]. In signaling circuits that exhibit FCD, the cells' response to extracellular gradients is more sensitive to the relative change in ligand concentration and less sensitive to the background ligand level.

Previous work has shown that RTK pathways perform relative sensing when sensing temporal gradients in ligand concentrations [39]. Similar to temporal gradient sensing, the ARP, a measure of cells' ability to detect spatial gradients, also exhibits FCD (Figure 5A). The ARP is linearly proportional to the relative gradient g (inset of Figure 5A), a phenomena often known as the Weber-Fechner law [38]. Notably, the range over which ARP exhibits FCD is limited to an order of magnitude in ligand concentration. Interestingly, this range is extended with increasing rate of preferential degradation (dashed black line in Figure 5B), however the increase is modest. The limited range of relative sensing is likely due to the narrow ligand-sensitivity region of the pathway. Notably, requiring receptor oligomerization prior to activation is a common signaling motif to extend the ligand-sensitivity region of the pathway, potentially broadening the range of relative sensing. Indeed, when dimerization is included in our model (see figure S2A), the relative sensing range is significantly extended with an increase in the preferential degradation of activated receptors (Figure 5B).

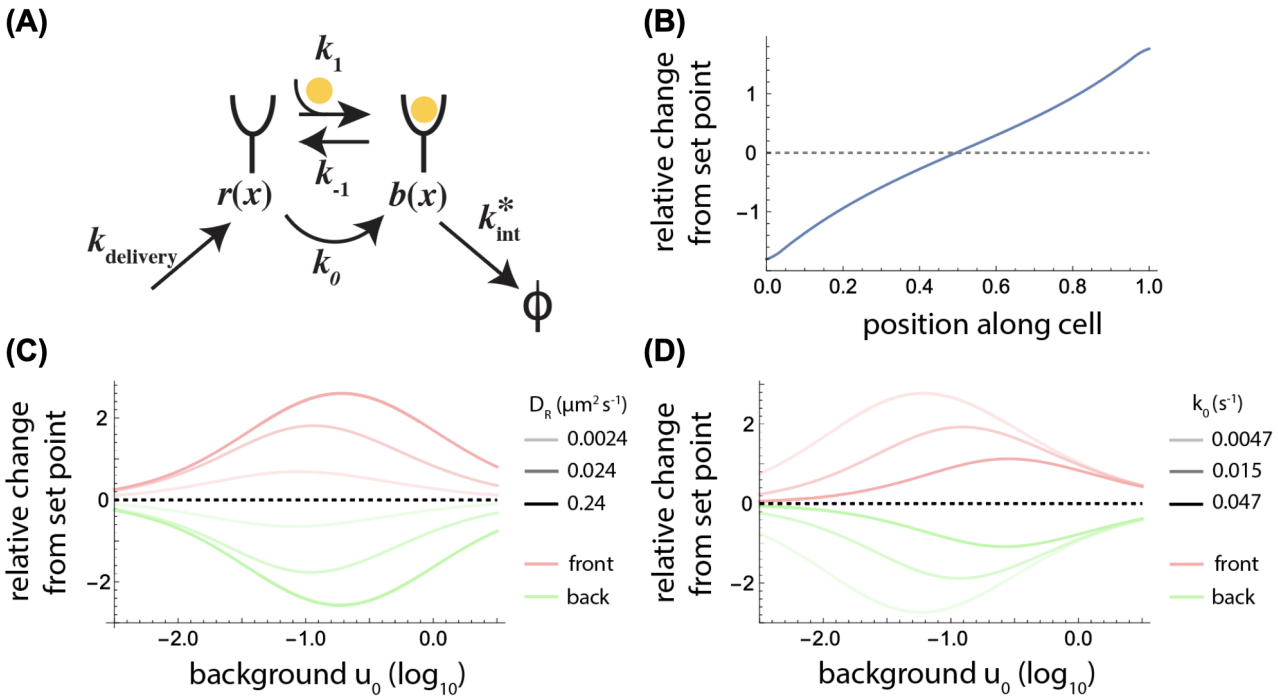

FIG. 6. **Gradient detection in perfectly adaptive LAGS model.** (A and B) The response at the leading edge (red) and trailing edge (green) of the cell. Values are reported relative to the ligand independent set point (dashed black line). The impacts of diffusion (A) and basal activation rate (B) are shown. Here we set $D_B = D_R$, $k^*_{\text{int}} = 10^{-2.5}s^{-1}$, $k_{-1} = 10^{-0.52}s^{-1}$. Unless stated otherwise, we set $k_0 = 10^{-1.82}s^{-1}$ and $D_R = 10^{-1.62}\mu m^2 s^{-1}$. We have used $u_0 = 0.1$, and $g = 10\%$

F. LAGS endow cells with a sense of absolute directions

Receptor polarization is a key component of spatial chemosensing by eukaryotic cells which can be defined as the cells' ability to identify regions of high ligand concentration from those of low ligand concentration [15]. Absolute identification of gradient direction requires cells to detect how local receptor activity along the membrane compares to the average activity, thereby allowing local regions to ascertain their relative position within the chemical gradient.

In the *standard model* of eukaryotic chemotaxis, the so called Local Excitation Global Inhibition (LEGI) framework [4, 18–20, 49, 50], the comparison between local and global activation profiles is achieved through an incoherent feedforward loop comprising a slowly diffusing excitatory species which encodes the local signal, a rapidly diffusing inhibitory species which encodes the average signal along the cell, and a downstream effector molecule which reads out the difference between the two. This network endows the effector with two important traits. First, the effector *perfectly adapts* [51] to spatially uniform ligand input. This allows the effector to encode a set point that is independent of extracellular ligand concentration. Second, the local effector levels are maintained above or below this set point based on whether the local ligand concentration is higher or lower than the average ligand concentration respectively. Downstream processes may then be tuned to subtract the set point, allowing for asymmetric engagement of these processes based on relative differences in signal along the cell.

The LEGI framework requires multiple molecules (an inhibitor, an activator, and an effector) to compare local and average signal condition. In contrast, a small modification of the LAGS model accomplishes absolute directional sensing through the combined effects of receptor diffusion and active receptor degradation. To do so, we develop an idealized perfectly adapting counterpart of our reaction diffusion model (Figure S2B). In the modified model, steady state of inactive receptors in the absence of any ligand is maintained not through their internalization but through their basal turnover to the active state and subsequent degradation. Specifically, we introduce basal activation of inactive receptors in the absence of any ligand. Notably, many RTKs and GPCRs are known to have a basal activation [40, 41]. It is easy to check that such a model is perfectly adaptive (see Supplementary Materials).

Similar to the LEGI model, the perfectly adapting LAGS model has an emergent set point in receptor activity that is determined by model parameters but is crucially independent of the ligand concentration. The local response along the membrane differs from this set point based on the impact of diffusion on the local receptor levels. Regions of the cell experiencing relatively high ligand concentration will have lower local receptor levels, thus

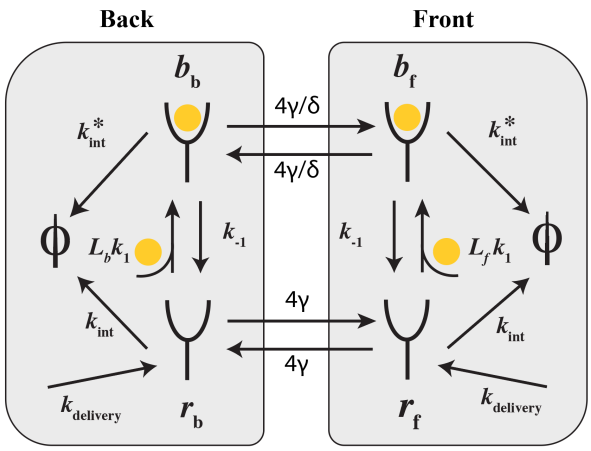

FIG. 7. **A simplified analytical model for receptor polarization.** Simplified two compartment model used for analytical steady state calculations. The factor of 4 acting on the diffusion terms results from the discretization process as previously described [52].

benefitting from diffusion and leading to a local response above the set point as desired (Figure 6B). Conceptually LAGS is endowed with a principle of chemosensing which does not rely on the diffusion differences that are an essential component of LEGI. In LAGS, chemosensing arises from ligand-driven depletion of receptors combined with receptor diffusion. Beyond its novel mechanistic underpinnings, such a sensing strategy is notable for its simplicity, potentially encoded in a single molecular species with active and inactive states.

G. A simplified model provides an analytical description of LAGS

The results presented above can be understood using a simple model that can be analytically solved. In the simple model, we coarse grain the one dimensional cell surface using two compartments that represent the front and the back of the cell. We describe the flow of receptors between these two compartments using mass action kinetics (Figure 7). While this model is analytically solvable, an interpretable expression for ARP is obtained when we assume rapid ligand dissociation ($\mu \to \infty$) and shallow gradient ($g \approx 0$):

$$\mathrm{ARP} = b_{\mathrm{Front}} - b_{\mathrm{Back}} = \frac{(8\gamma+1)gu_0}{(\beta u_0+1)(8\gamma+u_0(\beta+\frac{8\gamma}{\delta})+1)}. \tag{5}$$

The background ligand level that gives the optimal response (see Figure 5A) is given by

$$u_{\mathrm{opt}} = \sqrt{\frac{8\gamma+1}{\beta^2+\frac{8\beta\gamma}{\delta}}}. \tag{6}$$

. Evaluating Equation 5 at u_{opt} leads to an analytical description of the ARP which agrees quantitatively with the numerical simultations of the reaction diffusion model (Figure S2).

We further use this analytical model to understand the role of different processes in modulating ARP. To that end, we consider ARP_n: the ARP normalized by the ARP without diffusion ($\gamma \ll 1$, see Figure 2A). As the dependence of ARP_n on model parameters is complex, we will restrict our analysis to the limits of slow and rapid diffusion. In the limit of slow diffusion we find:

$$\mathrm{ARP}_n \approx 1 + 4\gamma\left(1-\frac{1}{\beta\delta}\right), \text{ for } \gamma \ll 1. \tag{7}$$

When diffusion is slow and $\beta\delta >> 1$, the ARP_n is sensitive to γ, but not β or δ. This explains both the observed lack of impact of δ on ARP when γ was low (left side of Figure 3A, note $\beta = 40$) and how ARP becomes insensitive to δ when β is large (Figure 3B).

When $\gamma \gg 1$, we have

$$\lim_{\gamma\to\infty} \mathrm{ARP}_n = \frac{4\beta}{\left(\sqrt{\beta}+\sqrt{\delta^{-1}}\right)^2}. \tag{8}$$

Similar to Eq. 7, eq. 8 captures essential features of our model. First, at high diffusion, higher β values lead to higher ARP (Figure 2). Second, δ increases ARP when γ is high *but* when β is modest (right side of Figure 3A). Finally, similar to the slow diffusion case, ARP is insensitive to β and δ when either is sufficiently large.

H. Kinetic parameters for eukaryotic signaling networks are consistent with LAGS

While careful estimation of relevant kinetic parameters that dictate the relevance of LAGS to specific signaling networks is cumbersome, previous work on RTKs and GPCRs provides an order of magnitude estimate for the dimensionless parameters defined in this study. Specifically, length of mammalian cells is typically $l_C \approx 20\mu m$ [43], the diffusion constants of cell surface receptors range between $D \approx 0.005 - 0.25\mu m^2 s^{-1}$ [34–37], with active receptors diffusing at rates $2-5$ lower compared to inactive receptors [35–37], the basal internalization rate of inactive receptors is $k_{\mathrm{int}} \approx 10^{-4}s^{-1}$ [26], and the rate internalization of active receptors is $k^*_{\mathrm{int}} \approx 10^{-3}$ [26, 39, 53]. Finally, ligand dissociation rates are typically $k_{-1} \approx 10^{-2}s^{-1}$ [39, 47, 54]. Based on these ranges, the dimensionless quantities evaluate to $\gamma \approx 0.75$, $\delta \approx 2$, $\beta \approx 10$, and $\mu \approx 100$. These numbers closely match the range of parameters used in our study. Importantly, this suggests that many eukaryotic signaling networks are be able to effectively polarize active receptors in response to extracellular ligand gradients.

III. DISCUSSION

The ability of cells to develop polarized responses under spatial gradients of extracellular ligands is a key feature of many eukaryotic cell behaviors. The first step in polarized response by eukaryotic cells is polarization of ligand-sensing receptors. Therefore, it is crucial to understand how processes at the plasma membrane, e.g. receptor diffusion and trafficking, affect receptor polarization. To that end, we developed a reaction diffusion model which revealed a novel polarization principle; Localized Activity Global Sensitization (LAGS). Counterintuitively, LAGS uses lateral diffusion and receptor degradation, processes that are *prima facie* detrimental to maintaining response polarity to enhance it. In LAGS, sensitivity to extracellular ligands is equalized along the membrane by lateral receptor diffusion while local receptor activity is protected from diffusing through rapid deactivation (through degradation or through rapid unbinding). We showed how LAGS increases active receptor polarization with stronger effects arising from higher levels of diffusion and preferential degradation (Figure 2). We found that LAGS endows signaling networks with fold change detection (Figure 5A), and explored how the range of detection may be increased through dimerization, receptor expression, and preferential degradation (Figure 5B). Furthermore, we found that when combined with a perfectly adaptive receptor model, LAGS results in a novel strategy for sensing absolute directions (Figure 6).

There are several ways to experimentally test LAGS. The most straightforward is the ability of cells to detect fold changes in ligand concentrations (Fold Change Detection or FCD). One cellular phenotype that may perform FCD is chemotaxis. Here, one can quantify chemotactic response (e.g. the chemotactic index) across different background ligand concentrations and different relative gradients. LAGS predicts that the same relative gradient will lead to similar chemotactic indices across different background ligand levels. Signaling networks such as the EGF/EGFR pathway that are known to perform FCD in temporal ligand gradients [39] will be an ideal system for these experiments. Moreover, given that EGFRs dimerize prior to activation, the range of background ligand concentrations over which relative sensing is exhibited can be tuned by changing receptor expression (Figure 5B).

The central parameters in LAGS; diffusion and degradation can be modulated using pharmacological perturbations. For example drugs such as latrunculin A [55] and jasplakinolide [56] target actin filaments and alter the diffusion of membrane proteins [34] and drugs like dynasore [57] that block clathrin mediated endocytosis, a first step in degradation of activated receptors. However, it should be noted that pharmacological perturbations often have unwanted off-target effects [58, 59]. Careful controls must be designed to account for these effects.

In our model, preferential degradation of active receptors plays a key role in polarization. Preferential degradation can be represented as an integral feedback controller [51]. Consequently, other forms of integral feedback motifs may also be employed. Other examples of the integral feedback motif [60] include chemical modifications such as methylation used in the *E. coli* chemotactic network [61] and activity induced inactivation often seen in G protein coupled receptors [62, 63] and ligand-gated ion channels [64]. Therefore, it is likely that LAGS applies to directional sensing by networks that rely on other forms of integral feedbacks. Finally, we note that while we focused our work on receptors, the LAGS applies to signaling components that receive spatially inhomogeneous inputs, diffuse, and are under an integral feedback control.

We therefore believe that LAGS may be useful to interpret a wide variety of directionally asymmetric behavior such as chemotropic [23, 65, 66] and chemotactic responses [4, 18–20, 49, 50].

IV. ACKNOWLEDGMENT

PD and AG acknowledge support from NIH grant R35GM142547.

[1] H. C. Berg, ed., *E. coli in Motion*, Biological and Medical Physics, Biomedical Engineering (Springer New York).

[2] J. P. Moore and T. Emonet, Current Biology **34**, R972 (2024).

[3] R. A. Arkowitz, Cold Spring Harbor perspectives in biology **1**, a001958 (2009).

[4] H. Levine, D. A. Kessler, and W.-J. Rappel, Proceedings of the National Academy of Sciences **103**, 9761 (2006).

[5] A. Bagorda and C. A. Parent, Journal of cell science **121**, 2621 (2008).

[6] K. F. Swaney, C.-H. Huang, and P. N. Devreotes, **39**, 265.

[7] A. Wodarz, Nature cell biology **4**, E39 (2002).

[8] D. M. Bryant and K. E. Mostov, Nature reviews Molecular cell biology **9**, 887 (2008).

[9] W. Bialek and S. Setayeshgar, Proceedings of the National Academy of Sciences **102**, 10040 (2005).

[10] F. Tostevin, P. R. Ten Wolde, and M. Howard, PLoS computational biology **3**, e78 (2007).

[11] V. Sourjik and N. S. Wingreen, Current opinion in cell biology **24**, 262 (2012).

[12] Y. Tu, Annual review of biophysics **42**, 337 (2013).

[13] H. H. Mattingly, K. Kamino, B. B. Machta, and T. Emonet, Nature physics **17**, 1426 (2021).

[14] A. Kashyap, W. Wang, and B. A. Camley, Biophysical Journal **123**, 1184 (2024).

[15] C. A. Parent and P. N. Devreotes, **284**, 765.
[16] D. Ghose, T. Elston, and D. Lew, **51**, 431.
[17] A. Narang, K. Subramanian, and D. Lauffenburger, Annals of biomedical engineering **29**, 677 (2001).
[18] A. Levchenko and P. A. Iglesias, Biophysical journal **82**, 50 (2002).
[19] H. Levine and W.-J. Rappel, Physics today **66**, 24 (2013).
[20] A. Mugler, A. Levchenko, and I. Nemenman, Proceedings of the National Academy of Sciences **113**, E689 (2016).
[21] J. Varennes, H.-r. Moon, S. Saha, A. Mugler, and B. Han, PLoS computational biology **15**, e1006961 (2019).
[22] H.-r. Moon, S. Saha, A. Mugler, and B. Han, Iscience **24** (2021).
[23] R. LeFebre, J. A. Landsittel, D. E. Stone, and A. Mugler, Physical Review Letters **133**, 138402 (2024).
[24] H. Nguyen, P. Dayan, and G. Goodhill, Journal of The Royal Society Interface **12**, 20141097 (2015).
[25] V. Lakhani and T. C. Elston, PLoS computational biology **13**, e1005386 (2017).
[26] H. S. Wiley, The EGF Receptor Family , 81 (2003).
[27] A. Sorkin and L. K. Goh, Experimental cell research **315**, 683 (2009).
[28] R. Irannejad and M. Von Zastrow, Current opinion in cell biology **27**, 109 (2014).
[29] R. Sulahian, O. Cleaver, and L. J.-s. Huang, **113**, 5287.
[30] J. Claudinon, M.-N. Monier, and C. Lamaze, **89**, 735.
[31] A. W. Gagnon, L. Kallal, and J. L. Benovic, Journal of Biological Chemistry **273**, 6976 (1998).
[32] P. Tsao, T. Cao, and M. von Zastrow, Trends in pharmacological sciences **22**, 91 (2001).
[33] K. Roepstorff, L. Grøvdal, M. Grandal, M. Lerdrup, and B. van Deurs, Histochemistry and cell biology **129**, 563 (2008).
[34] S. Lee, H. Y. Tan, I. I. Geneva, A. Kruglov, and P. D. Calvert, Journal of Cell Biology **217**, 2831 (2018).
[35] D. M. Freed, N. J. Bessman, A. Kiyatkin, E. Salazar-Cavazos, P. O. Byrne, J. O. Moore, C. C. Valley, K. M. Ferguson, D. J. Leahy, D. S. Lidke, *et al.*, Cell **171**, 683 (2017).
[36] M. Yanagawa, M. Hiroshima, Y. Togashi, M. Abe, T. Yamashita, Y. Shichida, M. Murata, M. Ueda, and Y. Sako, Science Signaling **11**, eaao1917 (2018).
[37] K. C. Mudumbi, E. A. Burns, D. J. Schodt, Z. O. Petrova, A. Kiyatkin, L. W. Kim, E. M. Mangiacapre, I. Ortiz-Caraveo, H. R. Ortiz, C. Hu, *et al.*, Cell reports **43** (2024).
[38] M. Adler and U. Alon, **8**, 81.
[39] E. Lyashenko, M. Niepel, P. D. Dixit, S. K. Lim, P. K. Sorger, and D. Vitkup, Elife **9**, e50342 (2020).
[40] M. Zeghal, G. Laroche, J. D. Freitas, R. Wang, and P. M. Giguère, Nature Communications **14**, 3684 (2023).
[41] G. Guo, K. Gong, B. Wohlfeld, K. J. Hatanpaa, D. Zhao, and A. A. Habib, Cancer research **75**, 3436 (2015).
[42] B. A. Schodin, T. J. Tsomides, and D. M. Kranz, Immunity **5**, 137 (1996).
[43] R. Milo, P. Jorgensen, U. Moran, G. Weber, and M. Springer, Nucleic acids research **38**, D750 (2010).
[44] P. Cumming, Synapse **65**, 892 (2011).
[45] T. Shi, M. Niepel, J. E. McDermott, Y. Gao, C. D. Nicora, W. B. Chrisler, L. M. Markillie, V. A. Petyuk, R. D. Smith, K. D. Rodland, *et al.*, Science Signaling **9**, rs6 (2016).
[46] R. Lee, S. Walker, K. Savery, D. Frank, and S. Gaudet, **53**, 867.
[47] J. Berkers, P. v. B. en Henegouwen, and J. Boonstra, Journal of Biological Chemistry **266**, 922 (1991).
[48] R. Karmakar, M.-H. Tang, H. Yue, D. Lombardo, A. Karanam, B. A. Camley, A. Groisman, and W.-J. Rappel, Physical Review E **103**, 012402 (2021).
[49] H. Meinhardt, **112**, 2867.
[50] P. A. Iglesias and P. N. Devreotes, **20**, 35.
[51] T. Friedlander and N. Brenner, Proceedings of the National Academy of Sciences **106**, 22558 (2009).
[52] D. Bernstein, **71**, 041103.
[53] J. A. Koenig and J. M. Edwardson, Trends in pharmacological sciences **18**, 276 (1997).
[54] W. W. Chen, B. Schoeberl, P. J. Jasper, M. Niepel, U. B. Nielsen, D. A. Lauffenburger, and P. K. Sorger, Molecular systems biology **5**, 239 (2009).
[55] I. Fujiwara, M. E. Zweifel, N. Courtemanche, and T. D. Pollard, Current Biology **28**, 3183 (2018).
[56] A. Holzinger, Cytoskeleton methods and protocols , 71 (2010).
[57] T. Kirchhausen, E. Macia, and H. E. Pelish, Methods in enzymology **438**, 77 (2008).
[58] L. M. Fujimoto, R. Roth, J. E. Heuser, and S. L. Schmid, Traffic **1**, 161 (2000).
[59] G. Preta, J. G. Cronin, and I. M. Sheldon, Cell Communication and Signaling **13**, 1 (2015).
[60] P. D. Dixit, A. Goetz, and R. R. Madsen, bioRxiv , 2024 (2024).
[61] T.-M. Yi, Y. Huang, M. I. Simon, and J. Doyle, Proceedings of the National Academy of Sciences **97**, 4649 (2000).
[62] H. Shankaran, H. S. Wiley, and H. Resat, BMC systems biology **1**, 1 (2007).
[63] E. Kelly, C. P. Bailey, and G. Henderson, British journal of pharmacology **153**, S379 (2008).
[64] M. Gielen and P.-J. Corringer, The Journal of Physiology **596**, 1873 (2018).
[65] M. Tessier-Lavigne, M. Placzek, A. G. Lumsden, J. Dodd, and T. M. Jessell, Nature **336**, 775 (1988).
[66] X. Li, S. Shim, K. R. Hardin, K. G. Vanaja, H. Song, A. Levchenko, G.-l. Ming, and J. Q. Zheng, Molecular and Cellular Neuroscience **123**, 103772 (2022).

V. SUPPLEMENTARY MATERIALS

All calculations described in this work were performed in Mathematica. The notebooks are available at https://github.com/adgoetz186/Chemosensing

A. The model with basal receptor activity is perfectly adaptive

In the main text, we introduced a model with basal receptor activation (Figure S2B) as a model exhibiting perfect adaptation. The equations describing the evolution of concentrations of chemical species in this model under uniform ligand concentration are given by:

$$\frac{dR}{dt} = k_{\text{delivery}} - k_0 R + k_{-1} B - L k_1 R \tag{9}$$

$$\frac{dB}{dt} = k_0 R - k^*_{\text{int}} B - k_{-1} B + L k_1 R \tag{10}$$

Solving the above for steady state ($\frac{dR}{dt} = \frac{dB}{dt} = 0$) gives:

$$R = \frac{k_{\text{delivery}} \left(k^*_{\text{int}} + k_{-1}\right)}{k^*_{\text{int}} \left(k_0 + k_1 L\right)} \tag{11}$$

$$B = \frac{k_{\text{delivery}}}{k^*_{\text{int}}} \tag{12}$$

Note that in Eq. 12, the response B is independent of ligand input while the total number of receptors decrease with increasing ligand concentration. When combined with spatial ligand gradients and diffusion of receptors, the model results in diffusion removing receptors from the low ligand regions and supplementing the high ligand regions leading to the deflections in response required of a gradient detection circuit.

B. ⟨ARP⟩ quantifies polarization in receptor activity over optimal background range

The active receptor polarization (ARP) is defined as the difference in active receptor concentration at the leading edge and the trailing edge of the cell. Notably, in addition to model parameters, ARP depends on background ligand concentration u_0. We observe that ARP= $b(1) - b(0)$ has a local maxima with respect to background ligand concentration u_0 at a concentration $u_0 = u_{\text{opt}}$. We define an average ARP (⟨ARP⟩) that averages over an order of magnitude of backgrounds centered about the optimal background for the specific set of parameters. We write the ⟨ARP⟩ as:

$$\langle \text{ARP} \rangle = \int_{u_{\text{opt}}-0.5}^{u_{\text{opt}}+0.5} \left(b(1) - b(0)\right) du_0 \tag{13}$$

Where u_{opt} is the background which gives the maximum value of $b(1) - b(0)$. Both u_{opt} and u_0 are in the $\log_{10}$ scale.

We also quantify the relative difference between leading edge response relative to the trailing edge response which we call the relative ⟨ARP⟩. This value is defined as follows,

$$\langle \text{relative ARP} \rangle = \int_{u_{\text{opt}}-0.5}^{u_{\text{opt}}+0.5} b(1)/b(0) du_0 \tag{14}$$

Here we keep our analysis in the region of maximum ARP so we keep the definition of u_{opt} used in Eq. 13. Both u_{opt} and u_0 are on the $\log_{10}$ scale.

For the calculation of both the ⟨ARP⟩ and the ⟨relative ARP⟩, we solve the reaction diffusion equations to obtain b(x), find u_{opt}, and calculate the integral from Eq. 13 or Eq. 14. These calculations are performed numerically in Mathematica.

C. Supplementary Figures

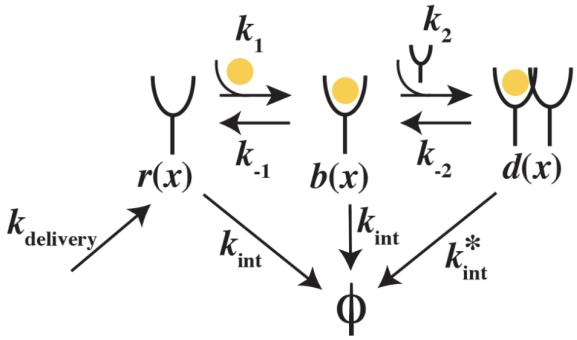

FIG. S1. **Dimer model.** (A) Model schematic with dimerization

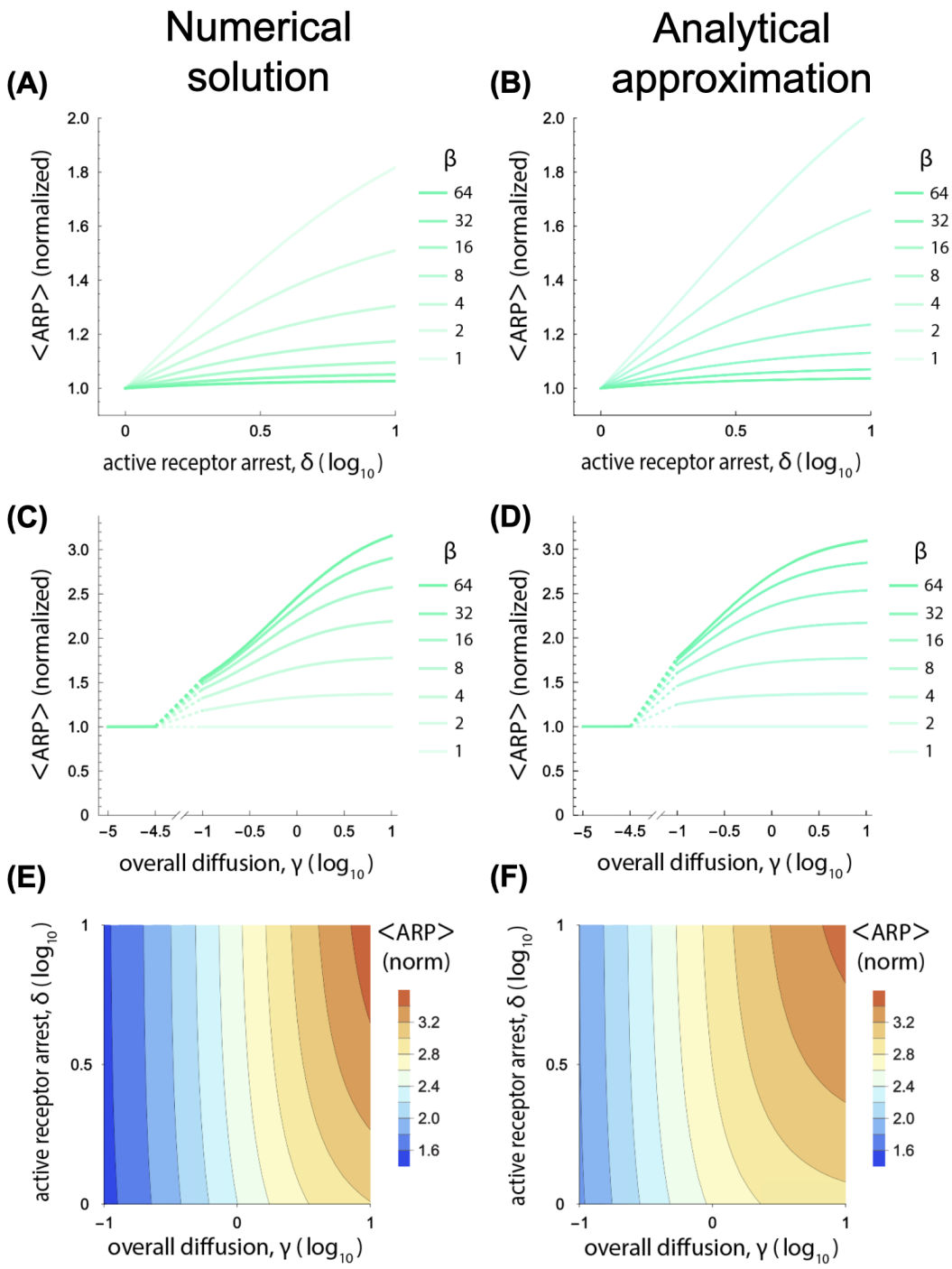

FIG. S2. **Comparison between Analytical model with true model simulation.** (A,C,E) True model simulations under high μ, $\mu = 10^7$. (B,D,F) Analytical model results. Unless stated otherwise we set $\gamma = 0.4$, $\delta = 1$, and $\beta = 40$.